Rheology, Crystallization Behaviors, and Thermal Stabilities of Poly(butylene succinate)/Pristine Multiwalled Carbon Nanotube Composites Obtained by Melt Compounding

Guoli Wang,[1] Baohua Guo,[1] Jun Xu,[1] Rui Li[2]

[1]*Department of Chemical Engineering, Institute of Polymer Science and Engineering, Tsinghua University, Beijing, People's Republic of China*
[2]*China Textile Industrial Engineering Institute, Beijing, People's Republic of China*

Received 14 May 2010; accepted 16 August 2010
DOI 10.1002/app.33222
Published online 16 February 2011 in Wiley Online Library (wileyonlinelibrary.com).

ABSTRACT: Poly(butylene succinate) (PBS)/pristine raw multiwalled carbon nanotube (MWCNT) composites were prepared in this work via simple melt compounding. Morphological observations indicated that the MWCNTs were well dispersed in the PBS matrix. Moreover, the incorporation of MWCNTs did not affect the crystal form of PBS as measured by wide-angle X-ray diffraction. The rheology, crystallization behaviors, and thermal stabilities of PBS/MWCNT composites were studied in detail. Compared with neat PBS, the incorporation of MWCNTs into the matrix led to higher complex viscosities ($|\eta^*|$), storage modulus (G'), loss modulus (G''), shear thinning behaviors, and lower damping factor (tan δ) at low frequency range, and shifted the PBS/MWCNT composites from liquid-like to solid-like, which affected the crystallization behaviors and thermal stabilities of PBS. The presence of a very small quantity of MWCNTs had a significant heterogeneous-nucleation effect on the crystallization of PBS, resulting in the enhancement of crystallization temperature, i.e., with the addition of 0.5 wt % MWCNTs, the values of T_c of PBS/MWCNT composites could attain to 90°C, about 6°C higher than that of neat PBS, whereas the values of T_c increased slightly with further increasing the MWCNTs content. The thermogravimetric analysis illustrated that the thermal stability of PBS was improved with the addition of MWCNTs compared with that of neat PBS. © 2011 Wiley Periodicals, Inc. J Appl Polym Sci 121: 59–67, 2011

Key words: poly(butylene succinate); multiwalled carbon nanotubes; rheology; crystallization behavior; thermal stability

INTRODUCTION

Biodegradable polymers have received much attention in fundamental research and technology because of their potential in environmental protection and biomedical applications. Among these polymers, poly(butylene succinate) (PBS) is a biocompatible linear aliphatic polyester, which is usually synthesized through the polycondensation reaction between succinic acid and 1,4-butanediol. PBS exhibits good biodegradability, melt processibility, thermal properties, and chemical resistance compared with other aliphatic polyesters, and these properties make it a potential and promising material in the fields of plastics and has been made into injection-molded products, films, and fibers.[1–4] However, softness, low melt viscosity, and slow crystallization rates have limited its processing and potential applications, particularly for injection molding. On the one hand, the lower melt viscosity is unsuitable for the processing properties of PBS. Also, for films and fibers preparation, the crystallization of PBS can be accelerated through drawing. However, in the case of injection molding, it is impossible to draw the molded plastics. If the crystallization rate is slow, the molding process needs longer time and results in a higher cost process. Therefore, it is very necessary to improve the performance of PBS. Different techniques, such as physical blending, chemical copolymerization, and nanocompounding have been explored to improve these performances.[5–11] Among these techniques, the incorporation of nanoinorganic fillers into PBS matrix is an efficient strategy to prepare composites with high performance. For example, Someya et al.[12] prepared PBS/clay nanocomposites by a simple melt blending, and showed that the addition of clay particle could increase the tensile modulus of PBS. Miyauchi et al.[13] investigated the degradation behaviors of PBS/TiO_2 nanocomposites and concluded that the incorporation of low content of fillers could enhance the degradation rate of PBS.

Correspondence to: B. Guo (bhguo@mail.tsinghua.edu.cn).
Contract grant sponsor: National Natural Science Foundation of China; contract grant number: 50673050.

In recent years, carbon nanotubes (CNTs) have been regarded as an effective one-dimensional reinforcing filler for preparing composites with high performance owing to its high flexibility, low mass density, and large aspect ratio.[14] Generally, polymer/MWCNT composites exhibit higher mechanical, thermal, and electronic properties than those of neat polymers, and these improved performances are usually based on the good dispersion of MWCNTs in the polymer matrix and strong interfacial interaction between MWCNTs and polymer. However, owing to the Van der Waals interactions between individual tubes, MWCNTs bundles are often formed, resulting in the poor dispersion states of MWCNTs into the polymer matrix, which in turn affect the physical properties of composites.[15] Thus, the well dispersion states of MWCNTs and good interaction effects between polymer and MWCNTs are very important for the enhancement on the properties of composites. Polymer/MWCNT composites with higher performances have been prepared by melt compounding techniques, which can provide high shear forces, resulting in the good interactions between MWCNTs and polymers.[16–18] For example, Ray et al.[19] prepared PBS/MWCNT nanocomposites by melt compounding and showed that the incorporation of 3 wt % MWCNTs could largely increase the mechanical and electrical properties of neat PBS. Also, Shih et al.[4] investigated the structure and properties of PBS/modified MWCNT composites obtained by melt compounding. It was shown that the electronic, thermal, and mechanical properties of neat PBS were enhanced with the addition of MWCNTs, which would be potentially useful in electronic packaging materials. In another work, Pramoda et al.[20] and Song and Qiu[21] have investigated the crystallization behaviors of PBS/MWCNT composites obtained by melt-blending, respectively, and concluded that MWCNTs could act as a significant heterogeneous-nucleation agent on the crystallization of PBS, leading to the enhancement in crystallization rate of PBS. In addition, Shih et al.[22] studied the thermal degradation kinetic of PBS/MWCNT nanocomposites and showed that the addition of MWCNTs could increase the heat and electrical conductivity of PBS. However, to the best of our knowledge, little work has been done about the effect of pristine raw MWCNTs on the rheological properties of PBS and the relation between microstructure and macroscopic properties of PBS/MWCNT composites, which is very important for the processing properties and potential application of neat PBS.

In this work, pristine MWCNTs were used without any pretreatment, and PBS/pristine MWCNT composites were prepared through simple melt compounding method, and the effect of pristine MWCNTs on the rheology, crystallization behaviors, and thermal stabilities of PBS were studied in detail with different techniques. The morphology and crystal form of PBS/MWCNT composites were investigated through scanning electron microscopy (SEM), transmission electron microscopy (TEM), and wide-angle X-ray diffraction (WAXD) analysis. The rheology, crystallization behaviors, and thermal stabilities were also investigated to study the effect of MWCNTs loading on the structure of PBS/MWCNT composites and the relation between microstructure and macroscopic properties of PBS/MWCNT composites.

EXPERIMENTAL

Materials and samples preparation

The multiwalled carbon nanotubes (MWCNTs) used in this work were prepared by chemical vapor deposition method and were obtained from the Green Reaction Engineering Laboratory of Tsinghua University, Beijing, China. Their length was about 10 μm, and the purity of CNTs produced was about 95%. CNTs were used as received, without any pretreatment. PBS was obtained from HeXing Chemical Corp., AnQing, China, and its melt flow index was 15 g/10 min at the temperature of 160°C. The melt blending of neat PBS with 0.5, 1, 2, and 3 wt % of MWCNTs were conducted using a mixer (HAAKE, RS600, German) at a temperature of 140°C for 10 min. PBS was dried at 60°C to remove water and some impurities before mixing. The samples obtained by melt mixing were used for compression for various measurements. Compression temperature was 150°C and pressure was 10 MPa (When the researchers do this experiment, especially for adding the MWCNTs into the polymer, the researchers must put on the gas mask and rubber glove to avoid sucking the MWCNTs into the body).

Characterization

SEM was used to examine the microstructure morphology of fractured surface of the samples. The images were observed under an acceleration voltage of 20 kV with a JSM-7401 for SEM experiment. TEM observations were also carried out to examine the microstructure morphology of the samples. Ultrathin sections of specimens were cut from the compressed sheets using a Ultramicrotome-LeiCa EM. The thin slices were put on copper grids and then observed on a JEM-2010 TEM with an acceleration voltage of 200 kV. WAXD analysis was carried out at room temperature using an X-ray diffractometer (Rigaku, D/max-RB) with Cu Kα radiation at a scanning rate of 6°/min. All rheological measurements were performed on a strain-controlled rheometer (Anton Paar, MCR301) using 25-mm diameter parallel plates at 140°C. Testing sample disks with a thickness of 1.5 mm and a diameter of 25 mm were prepared by

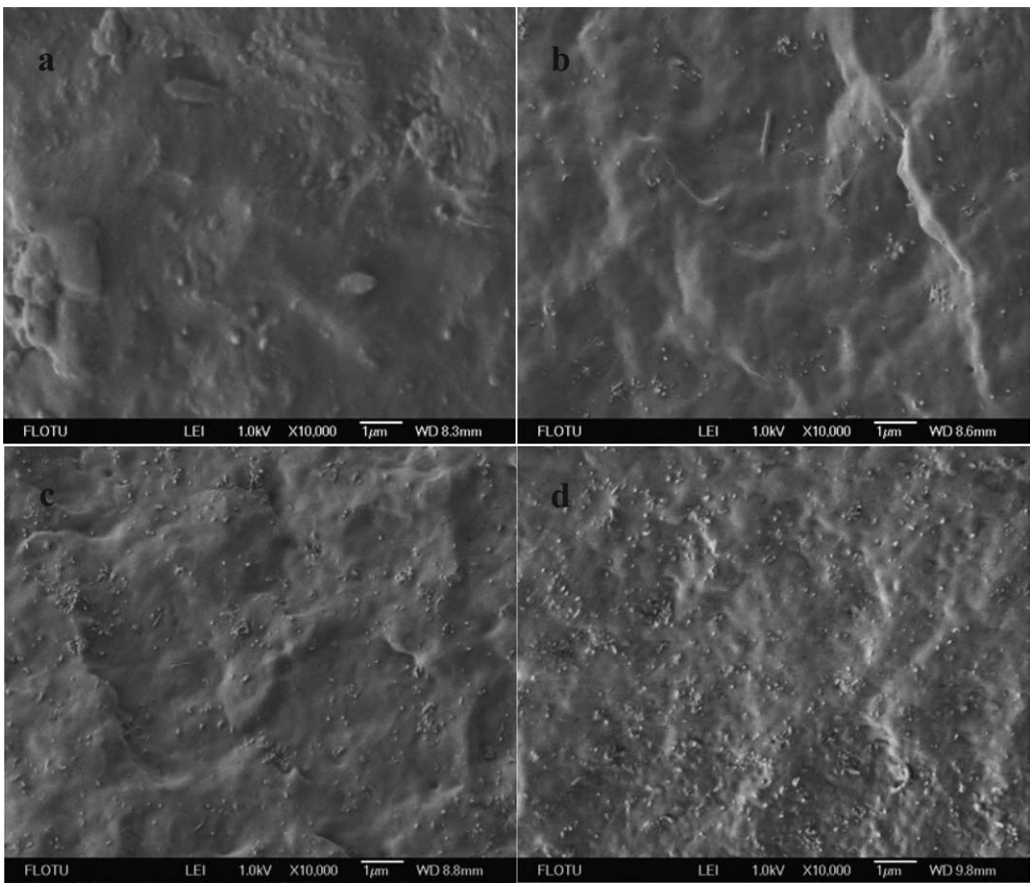

Figure 1 SEM images of the fractured surface of PBS/MWCNT composites with various MWCNTs loading: (a) 0.5 wt %, (b) 1 wt %, (c) 2 wt %, and (d) 3 wt %.

compression molding of the samples at 150°C for 8 min. Small-amplitude oscillatory shear ($\gamma = 0.5\%$) measurements were conducted within a frequency range from 0.05 to 120 rad/sec. DSC experiment was performed using a Shimadzu DSC-60 differential scanning calorimeter under nitrogen atmosphere in the temperature range from 30°C to 160°C. Neat PBS and PBS/MWCNT composites were scanned from 30°C to 160°C (Run I), retained at 160°C for 5 min to eliminate the thermal history, and then cooled to 30°C at a rate of 10°C/min, and after that the samples were reheated to 160°C at a rate of 10°C/min (Run II). Spherulite morphology of neat PBS and PBS/MWCNTs composites were observed using a polarizing optical microscope (Olympus BH-2). Thermogravimetric analysis was performed on a Shimadzu DTG-60 thermogravimetric analyzer by heating the samples to 550°C at a rate of 20°C/min under nitrogen atmosphere.

RESULTS AND DISCUSSION

Morphology of neat PBS and PBS/MWCNT composites

The morphology and dispersion states of MWCNTs in polymer matrix were investigated using SEM and TEM. Figure 1 shows the SEM images of fracture surfaces of PBS/MWCNT composites with different MWCNTs loading. It is clear from Figure 1(a) that the small amounts of MWCNTs are well dispersed and embedded in the PBS matrix without showing noticeable MWCNTs aggregates. With the increasing of MWCNTs content, the MWCNTs are homogeneously dispersed in the PBS matrix [Fig. 1(b,c)], which indicated that the MWCNTs are partly compatible with the PBS matrix. However, when the MWCNTs content increase to 3 wt %, as shown in Figure 1(d), small amounts of MWCNTs partly aggregates by themselves in the PBS matrix. The reason for this can be ascribed to the Van der Waals interaction between MWCNTs.[23] Also, the fracture surface of PBS/MWCNT composites is relatively smooth and the boundary between MWCNTs and PBS is not clear and showed that the MWCNTs are wrapped by PBS molecular chains and mixed well each other. TEM photos are generally used to characterize the dispersion state of MWCNTs in the PBS matrix at even higher magnification. Figure 2 shows the TEM images of ultrathin section of PBS/MWCNT composites with 2 wt % MWCNTs content. It is shown from Figure 2(a) that the individual MWCNT is

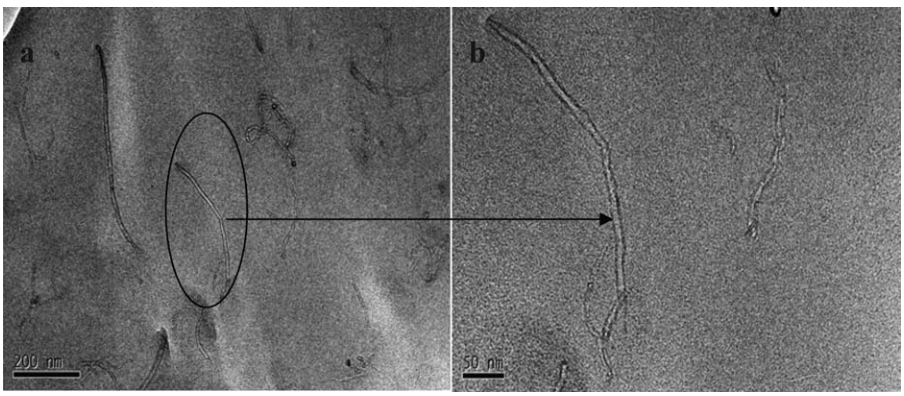

Figure 2 TEM images of the fractured surface of PBS/MWCNT composites with 2 wt % MWCNTs loading.

uniformly dispersed in the PBS matrix with a small quantity of aggregates because of the high shear forces applied by melt blending. Meanwhile, most MWCNTs are curved in the composites because of the flexibility of the MWCNTs. At higher magnification, it can be seen from Figure 2(b) that the individual MWCNT is regarded as a long hollow fiber with diameter around 20 nm and length below 1 μm. Moreover, it is very necessary to investigate the effect of pristine MWCNTs loading on the crystal form of neat PBS. Figure 3 shows the WAXD patterns of neat PBS and PBS/MWCNT composites with different MWCNTs content. It is clear that PBS/MWCNT composites exhibit the same diffraction peak locations as those of neat PBS, suggesting that the addition of pristine MWCNTs has almost no effect on the crystal form of neat PBS. The main peaks, which located at around $2\theta = 19.61°$, 21.92°, and 22.67°, were assigned to (020), (021), and (110) planes of the α form of PBS, respectively.[24]

Rheological properties

The complex viscosity ($|\eta^*|$), storage modulus (G'), loss modulus (G''), and damping factor (tan δ) of neat PBS and PBS/MWCNT composites as a function of frequency for a typical response are shown in Figure 4. It is clear from Figure 4(a) that the values of $|\eta^*|$ of neat PBS and PBS/MWCNT composites decrease with the increasing frequency, which indicates a non-Newtonian behavior over the whole frequency range. However, PBS/MWCNT composites exhibit higher $|\eta^*|$ values than those of neat PBS at low frequency and increase gradually with the increasing MWCNTs content. In addition, this reinforcement effect is more significant at low frequency than at high frequency and showed that the interconnected or network-like structures are formed, which may be due to the polymer–particle and particle–particle interactions.[25] The PBS/MWCNT composites exhibit a higher shear thinning behaviors than those of neat PBS, which is attributed to the orientation and entanglement of molecular chains during the applied shear force. To further study the effect of MWCNTs on the rheological properties of PBS/MWCNT composites, the shear thinning exponents (n) for flow process of PBS/MWCNT composites are described owing to the relationship of $|\eta^*| \approx \omega^n$,[26] and their results are summarized in Table I. It is clear that the shear thinning behavior of PBS/MWCNT composites largely depended on the content of MWCNTs; the higher the MWCNTs content, the stronger the shear thinning behaviors of PBS/MWCNT composites, and the n values of PBS/MWCNT composites decrease largely with the increasing MWCNTs content, which can be ascribed to the break down of network-like structures with increasing of the frequency.

The storage modulus (G') and loss modulus (G'') for neat PBS and PBS/MWCNT composites as a function of frequency are shown in Figure 4(b,c). The values of G' and G'' of neat PBS and PBS/MWCNT composites increase with increasing of the frequency, and this enhancement effect is more

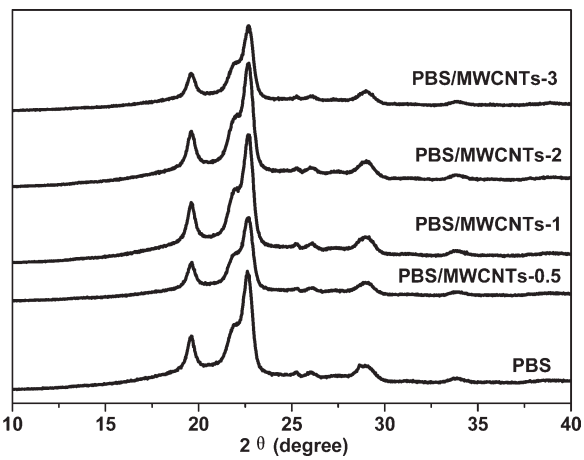

Figure 3 X-ray diffractograms of neat PBS and PBS/MWCNT composites.

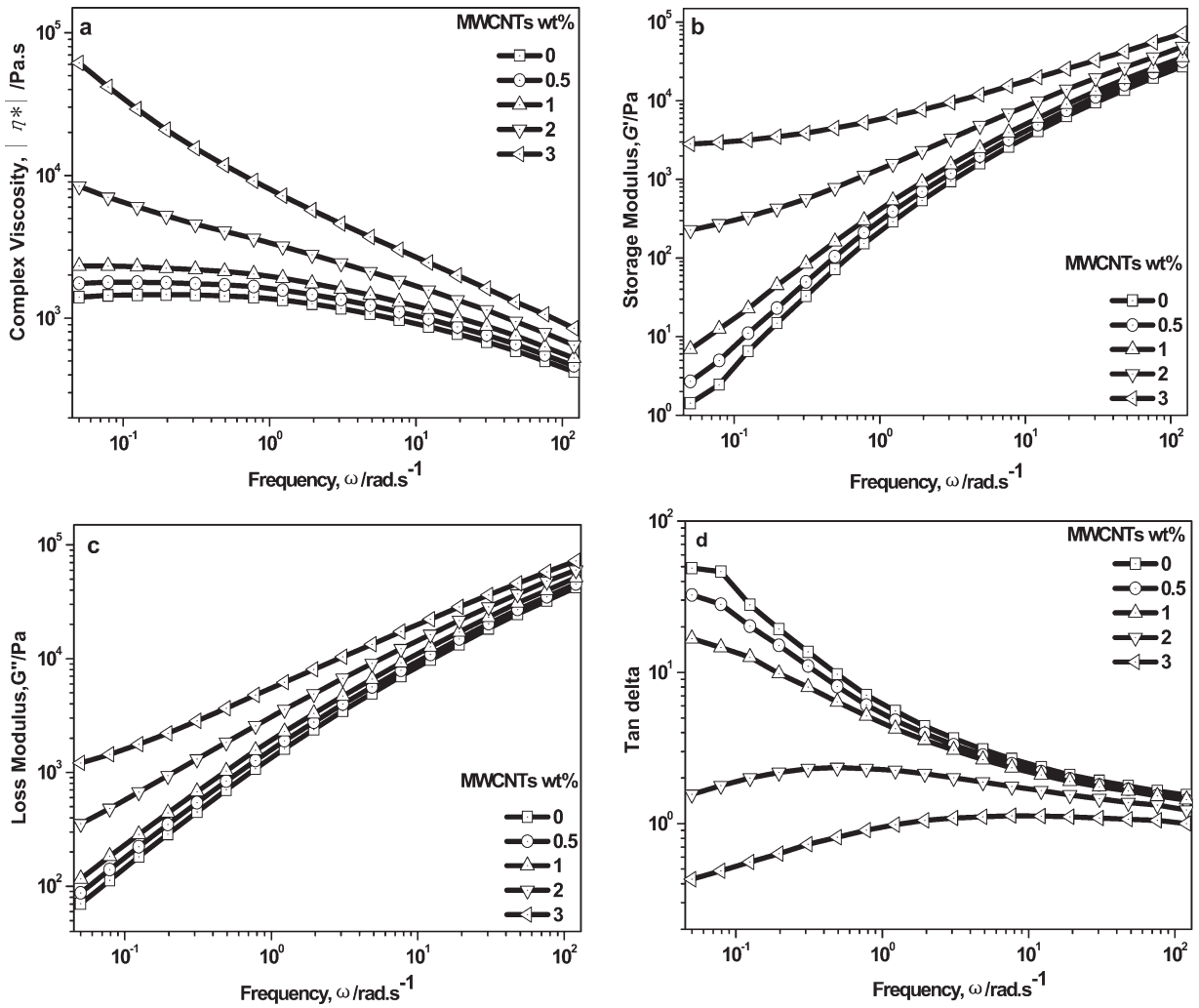

Figure 4 Dynamic complex viscosity (|η*|) (a), storage modulus (G') (b), loss modulus (G'') (c), and damping factor (tan δ) (d) as a function of frequency of neat PBS and PBS/MWCNT composites.

significant at low frequency. These results are very similar to the relaxation behaviors of the typical filled-polymer composites systems.[27,28] The slopes of the terminal region of G' and G'' for PBS/MWCNT composites are shown in Table I. It is clear that the slopes of G' and G'' for PBS/MWCNT composites decrease with increasing of the MWCNTs content, which can explain that the polymer–nanotube or nanotube–nanotube strong interactions result in the formation of network-like structure, leading to the pseudo solid-like behaviors of PBS/MWCNT composites.[29] Moreover, the values of G' and G'' of the PBS/MWCNT composites are higher than those of neat PBS and increase with increasing of MWCNTs loading, particularly at low-frequency region, indicating that the network structure is formed by the filler–filler and filler–polymer interaction in the presence of MWCNTs, leading to more elasticity than neat PBS. In addition, the PBS/MWCNT composites show almost similar or a little higher values of G' and G'' than that of neat PBS at high frequency and showed that the network structures are broken down under the effect of higher shear force.

The variation of tan δ with frequency for neat PBS and PBS/MWCNT composites is shown in Figure 4(d). It is clear that the value of tan δ decreases with the increasing MWCNTs contents and showed that the elastic properties are improved by incorporating the MWCNTs into PBS matrix. Moreover, the value of tan δ decreases with the increasing frequency, which may be due to the partial orientation of

TABLE I
Variations of Low-Frequency Slopes of (|η*|), G', and G'' versus ω of Neat PBS and PBS/MWCNT Composites

Samples	Slope of |η*| versus ω	Slope of G' versus ω	Slope of G'' versus ω
PBS	−0.01	1.72	0.98
PBS/MWCNTs-0.5	−0.03	1.59	0.96
PBS/MWCNTs-1	−0.06	1.38	0.93
PBS/MWCNTs-2	−0.29	0.61	0.73
PBS/MWCNTs-3	−0.67	0.25	0.52

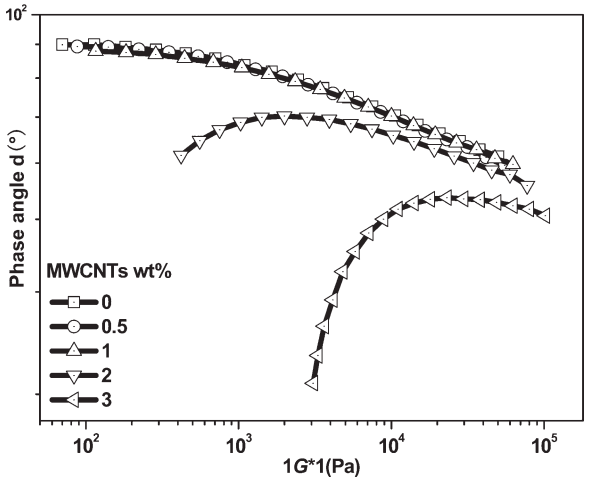

Figure 5 Plots of phase angle versus complex modulus of neat PBS and PBS/MWCNT composites.

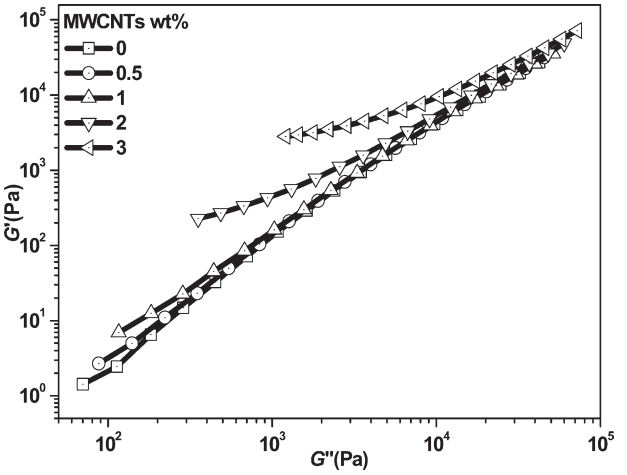

Figure 6 Plots of G' versus G'' for neat PBS and PBS/MWCNT composites.

polymer chains caused by shear. Interestingly, the values of the tan δ maximum of PBS/MWCNT composites shifted to higher frequency with the increasing MWCNTs content, indicating that the network structure was formed in the PBS/MWCNT composites.[30] The plots of the phase angle versus the absolute value of complex modulus for PBS/MWCNT composites, known as the Van Gurp–Palmen Plot,[31] are shown in Figure 5. It is clear that the phase angle of PBS/MWCNT composites decreased with the increasing complex modulus, and indicated that the incorporation of MWCNTs can enhance the elasticity of neat PBS. When the MWCNTs content is over 1 wt %, PBS/MWCNT composites showed smaller δ at lower values of complex modulus and decreased with the increasing MWCNTs content, and it can be concluded that the elastic properties of neat PBS were enhanced by the addition of MWCNTs, and this enhancement effect was more pronounced at higher MWCNTs content.

The plots of G'' versus G' for neat PBS and PBS/MWCNT composites are shown in Figure 6. It is well known that if the polymer melt is isotropic and homogeneous, the Cole–Cole plot provides a master curve with a slope of 2, irrespective of temperature.[32] However, PBS/MWCNT composites did not exhibit the single master curve, and the slopes of the curves in the terminal regime were less than 2 and decreased with the increasing MWCNTs content, and showed that PBS/MWCNT composites were heterogeneous and underwent some chain conformational changes because of the interconnected or network structures in the presence of MWCNTs. In addition, when the G'' value is over 10^4, the slope of PBS/MWCNT composites increased and attained a slope similar to that of neat PBS, indicating that the interconnected or network structures were destroyed by the higher shear force.

Crystallization behaviors

Figure 7 shows the DSC thermograms of first cooling and second heating for neat PBS and PBS/MWCNT composites, respectively. The related

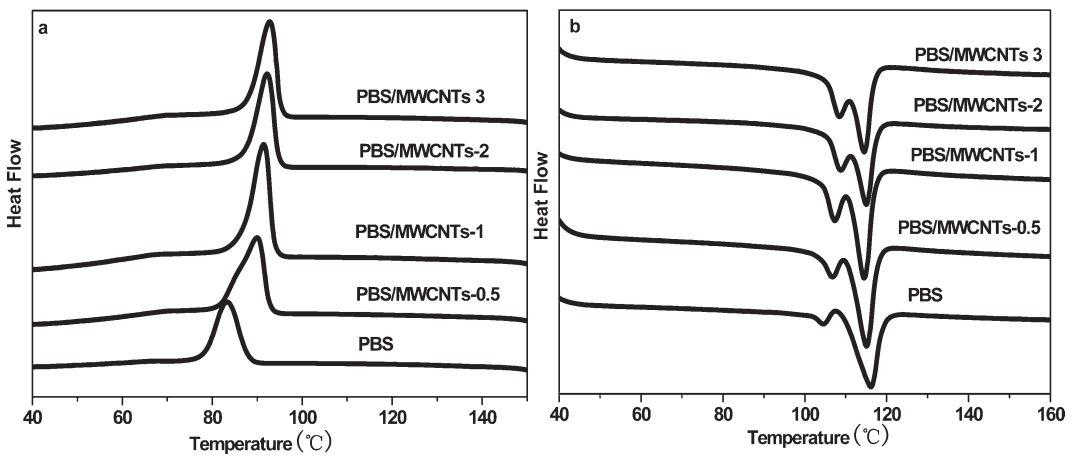

Figure 7 DSC curves of (a) the first cooling and (b) the second heating of neat PBS and PBS/MWCNT composites.

TABLE II
Thermal Properties of Neat PBS and PBS/MWCNT Composites

Samples	T_m(°C) I/II	ΔH_m (J/g)	T_c (°C)	X_c (%)
PBS	104.5/116.2	45.7	83.4	41.5
PBS/MWCNTs-0.5	106.8/115.1	53.1	90.0	48.3
PBS/MWCNTs-1	107.4/114.5	55.9	91.4	50.8
PBS/MWCNTs-2	108.9/115.0	51.9	92.2	47.2
PBS/MWCNTs-3	108.5/114.5	58.1	92.8	52.8

thermal data are summarized in Table II. From Figure 7(a) and Table II, it is clear that the crystallization temperature (T_c) of PBS/MWCNT composites were all higher than that of neat PBS and increased with the increase in the MWCNTs loading, indicating that the MWCNTs have heterogeneous-nucleation effects on the crystallization of PBS and promoted the crystallizability of PBS. Interestingly, we also noted that the value of T_c of PBS is increased by 6°C via adding only 0.5 wt % MWCNTs, whereas the T_c increased slowly with further increasing the MWCNTs content. These results showed that the nucleation effects were not proportional to the MWCNTs content, indicating that a saturation nucleation effect existed particularly at higher MWCNTs content. The reason for this can be concluded as follows: when the MWCNTs content is over 0.5 wt %, the rheological network is formed, leading to the decreased chain mobility of PBS and limited the crystallization behavior of PBS. Yang et al.[33] studied the crystallization behaviors of PPS/MWCNT nanocomposites and showed that the nucleation effects increased weakly with the increasing MWCNTs content. From Figure 7(b), it is shown that the melting peaks of PBS/MWCNT composites were all sharper than those of neat PBS, indicating that the crystal of PBS/MWCNT composites were more regular than those of neat PBS. In addition, two melting endotherms were found for both neat PBS and PBS/MWCNT composites, denoted as T_{m1} and T_{m2} from low to high temperatures, and these two melting peaks were attributed to the melting–recrystallization–remelting process of the lamellar, which has been reported for PBS and its copolymers.[34–36] The temperature and area of T_{m1} for the PBS/MWCNT composites were higher than those of neat PBS, and increased with the increasing MWCNTs content. They are probably connected with the melting point of original lamellae, whereas the temperature of T_{m2} was almost not affected by the incorporation of the MWCNTs, that is, the temperature of T_{m2} was similar to that of neat PBS, which was probable due to the melting point of the crystallites formed through the melting–recrystallization of the original lamellae during the DSC heating process. Moreover, it can be seen from Table II that the crystallinity degree (X_c) of PBS/MWCNT composites was higher than that of neat PBS, indicating that the incorporation of MWCNTs could slightly increase the crystallinity degree (X_c) of PBS.

The spherulite morphologies of neat PBS and PBS/MWCNT composites were also observed using polarizing optical microscope. The samples were

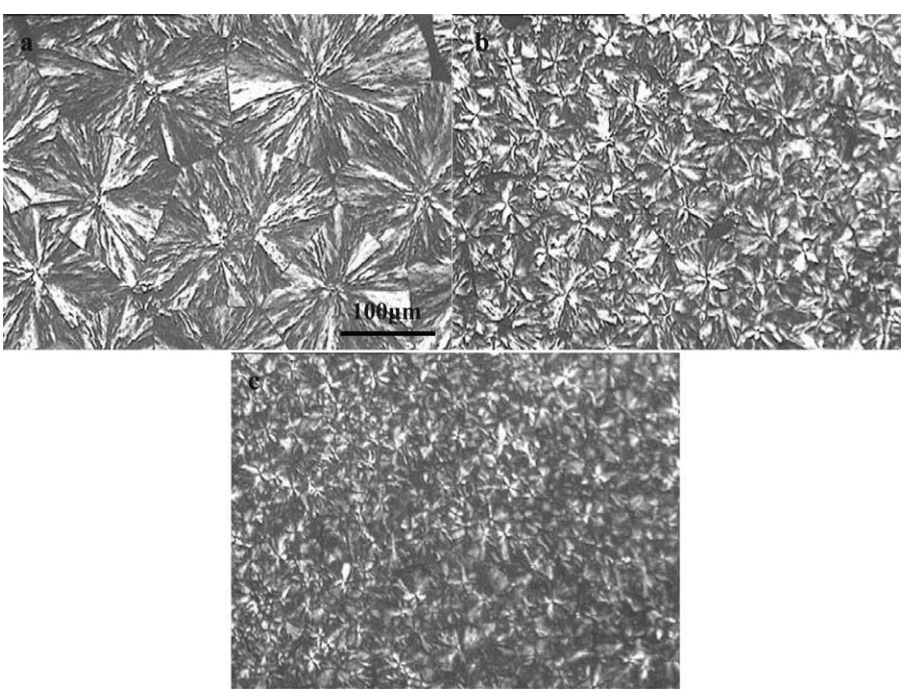

Figure 8 Polarized optical micrographs for PBS/MWCNT composites with (a) 0%, (b) 0.5%, and (c) 1% MWCNTs. These samples were all melt crystallized at 95°C.

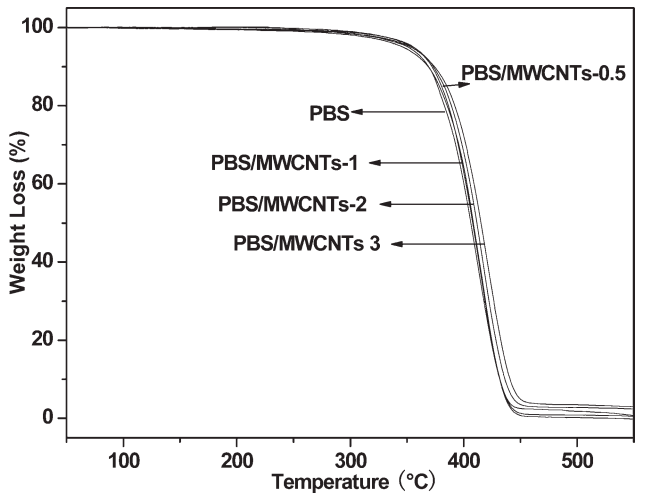

Figure 9 Thermogravimetric analysis curves of neat PBS and PBS/MWCNT composites.

pressed between two glass slides and melted at the temperature of 190°C for 5 min, followed by fast moving to the hot stage preliminarily set at 95°C for isothermal crystallizations. The corresponding microscopic photographs are shown in Figure 8. It is clear that the appearing spherulites are relatively big, and the spherulites boundaries can be clearly observed for neat PBS, whereas for the PBS/MWCNT composites, as shown in Figure 8(b,c), the spherulites size of PBS/MWCNT composites is smaller than that of neat PBS, and the spherulites boundaries are not clear with increasing MWCNTs content. These results suggest that the incorporation of MWCNTs increase the nuclei in system. The increased nuclei, of course, would induce more spherulites formation, many growing spherulites impinge each other, finally leading to the smaller spherulites size.[37]

Thermal stabilities

Thermogravimetric analysis was usually used to characterize the thermal stabilities of neat PBS and PBS/MWCNT composites, and their results are shown in Figure 9. It is clear that the incorporation of MWCNTs into the PBS matrix can slightly enhance the thermal degradation temperatures and the residual yields of neat PBS, and this enhancement effect was more significant with increasing MWCNTs content. For example, when the MWCNTs content is 0.5 wt %, the onset decomposition (at weight loss of 5%) is 356°C, about 5°C higher than that of neat PBS. This showed that the incorporation of MWCNTs can enhance the thermal stabilization of PBS matrix. The enhancement in the thermal stabilization might be ascribed to the good dispersion of MWCNTs in the PBS matrix; the well dispersion of MWCNTs into PBS matrix is probable to be an effective barrier effect to the volatile molecules produced from the PBS thermal decomposition. Similar result was also found in the PBS/functional MWCNT nanocomposite.[21]

CONCLUSIONS

Biodegradable PBS/pristine raw MWCNT composites were prepared through simple melt compounding method. The morphology of MWCNTs in the PBS matrix was observed by SEM and TEM, which indicated the well dispersion of MWCNTs in the PBS matrix. The WAXD results showed that the addition of MWCNTs had almost no effect on the crystal form of neat PBS. The rheology, crystallization behaviors, and thermal stabilities of PBS/MWCNT composites were performed to investigate the effect of the pristine MWCNTs on the structure and properties of neat PBS. The incorporation of MWCNTs into PBS matrix can lead to higher complex viscosities ($|\eta^*|$), storage modulus (G'), loss modulus (G''), shear thinning behaviors, and lower damping factor (tan δ) as measured by dynamic rheometer. The crystallization behaviors indicated that a small quantity of MWCNTs can effectively act as heterogeneous-nucleating agent, resulting in the enhancement on the crystallization temperature of neat PBS, i.e., with the addition of 3 wt % MWCNTs, the values of T_c of PBS/MWCNT composites can increase to 93°C, about 10°C higher than that of neat PBS. Moreover, the thermal stabilities of PBS/MWCNT composites are higher than those of neat PBS.

References

1. Pan, P. J.; Inoue, Y. S. Prog Polym Sci 2009, 34, 605.
2. Fujimaki, T. Polym Degrad Stab 1998, 59, 209.
3. Liu, L. F.; Yu, J. Y.; Cheng, L. D.; Yang, X. J. Polym Degrad Stab 2009, 94, 90.
4. Shih, Y. F.; Chen, L. S.; Jeng, R. J. Polymer 2008, 49, 4602.
5. Chen, G. X.; Kim, H. S.; Kim, E. S.; Yoon, J. S. Polymer 2005, 46, 11829.
6. Shibata, M.; Inoue, Y.; Miyoshi, M. Polymer 2006, 47, 3557.
7. Pepic, D.; Zagar, E.; Zigon, M.; Krzan, A.; Kunaver, M.; Djonlagic, J. Eur Polym J 2008, 44, 904.
8. Xu, Y. X.; Xu, J.; Liu, D. H.; Guo, B. H.; Xie, X. M. J Appl Polym Sci 2008, 109, 1881.
9. Xu, Y. X.; Xu, J.; Guo, B. H.; Xie, X. M. J Polym Sci Part B: Polym Phys 2007, 45, 420.
10. The, D. T.; Yoshii, F.; Nagasawa, N.; Kume, T. J Appl Polym Sci 2004, 91, 2122.
11. Bhatia, A.; Gupta, R. K.; Bhattacharya, S. N.; Choi, H. J. J Appl Polym Sci 2009, 114, 2837.
12. Someya, Y.; Nakazato, T.; Teramoto, N.; Shibata, M. J Appl Polym Sci 2004, 91, 1463.
13. Miyauchi, M.; Li, Y. J.; Shimizu, H. Environ Sci Technol 2008, 42, 4551.
14. Zhao, Y. Y.; Qiu, Z. B.; Yang, W. T. Compos Sci Technol 2009, 69, 627.
15. Thostenson, E. T.; Ren, Z. F.; Chou, T. W. Compos Sci Technol 2001, 61, 1899.

16. Anand, K. A.; Agarwal, U. S.; Joseph, R. J Appl Polym Sci 2007, 104, 3090.
17. Yeh, J. T.; Yang, M. C.; Wu, C. J.; Wu, C. S. J Appl Polym Sci 2009, 112, 660.
18. Kim, J. Y. J Appl Polym Sci 2009, 112, 2589.
19. Ray, S. S.; Vaudreuil, S.; Maazouz, A.; Bousmina, M. J Nanosci Nanotechnol 2006, 6, 2191.
20. Pramoda, K. P.; Linh, N. T. T.; Zhang, C.; Liu, T. X. J Appl Polym Sci 2009, 111, 2938.
21. Song, L.; Qiu, Z. B. Polym Degrad Stab 2009, 94, 632.
22. Shih, Y. F. J Polym Sci Part B: Polym Phys 2009, 47, 1231.
23. Lee, G. W.; Jagannathan, S.; Chae, H. G.; Minus, M. L.; Kumar, S. Polymer 2008, 49, 1831.
24. Ihn, K. J.; Yoo, E. S.; Im, S. S. Macromolecules 1995, 28, 2460.
25. Kim, J. Y.; Han, S. I.; Hong, S. P. Polymer 2008, 49, 3335.
26. Goad, M. A.; Potschke, P. J Non-Newtonian Fluid Mech 2005, 128, 2.
27. Krishnamoorti, R.; Giannelis, E. P. Macromolecules 1997, 30, 4097.
28. Krishnamoorti, R.; Vaia, R. A.; Giannelis, E. P. Chem Mater 1996, 8, 1728.
29. Ali, F. B.; Mohan, R. Polym Compos 2010, 31, 1309.
30. Kim, J. Y.; Kim, S. H. J Polym Sci Part B: Polym Phys 2006, 44, 1062.
31. Van, M. G.; Palmen, J. J Rheol Bull 1998, 67, 5.
32. Han, C. D.; Kim, J.; Kim, J. K. Macromolecules 1989, 22, 383.
33. Yang, J. H.; Xu, T.; Lu, A.; Zhang, Q.; Tan, H.; Fu, Q. Compos Sci Technol 2009, 69, 147.
34. Wang, X. H.; Zhou, J. J.; Li, L. Eur Polym J 2007, 43, 3163.
35. Yoo, E. S.; Im, S. S. J Polym Sci Part B: Polym Phys 1999, 37, 1357.
36. Qiu, Z. B.; Komura, M.; Ikehara, T.; Nishi, T. Polymer 2003, 44, 7781.
37. Xu, C. L.; Qiu, Z. B. Polym Adv Technol, to appear.